Monte Carlo studies of high-transverse-energy hadronic interactions

M. D. Corcoran
T. W. Bonner Nuclear Laboratories, Physics Department, Rice University, Houston, Texas 77251
(Received 9 October 1984; revised manuscript received 15 April 1985)

A four-jet Monte Carlo calculation has been used to simulate hadron-hadron interactions which deposit high transverse energy into a large-solid-angle calorimeter and limited solid-angle regions of the calorimeter. The calculation uses first-order QCD cross sections to generate two scattered jets and also produces beam and target jets. Field-Feynman fragmentation has been used in the hadronization. The sensitivity of the results to a few features of the Monte Carlo program has been studied. The results are found to be very sensitive to the method used to ensure overall energy conservation after the fragmentation of the four jets is complete. Results are also sensitive to the minimum momentum transfer in the QCD subprocesses and to the distribution of p_T to the jet axis and the multiplicities in the fragmentation. With reasonable choices of these features of the Monte Carlo program, good agreement with data at Fermilab/CERN SPS energies is obtained, comparable to the agreement achieved with more sophisticated parton-shower models. With other choices, however, the calculation gives qualitatively different results which are in strong disagreement with the data. These results have important implications for extracting physics conclusions from Monte Carlo calculations. It is not possible to test the validity of a particular model or distinguish between different models unless the Monte Carlo results are unambiguous and different models exhibit clearly different behavior.

I. INTRODUCTION

Since the CERN ISR experiments of the early 1970s,[1] there has been interest in the production of particles at high transverse momentum (p_T) in hadronic interactions. In the context of the quark-parton model, these high-p_T secondaries arise from the fragmentation of hard-scattered partons. These particles have limited momentum transverse to the direction defined by the parton's momentum and therefore form a "jet." The spectator partons in the beam and target particles form jets along the beam axis, giving an overall four-jet structure to the event.

The early experiments triggered on single particles at high p_T, but it was quickly realized that such a trigger would be subject to "trigger-bias" effects. That is, such a trigger would preferentially select events in which the fragmenting parton gave most of its momentum to a single particle, and the event sample selected in this way would be biased by the unknown fragmentation function.

Subsequent experiments used larger-solid-angle detectors to overcome trigger-bias effects. "Second-generation" jet experiments[2,3] used segmented calorimeters of ~ 2.5 sr center-of-mass (c.m.) solid angle and triggered on total transverse energy (E_T) deposited in the detector. However, arguments of trigger bias could still be made. It was hoped that even-larger-solid-angle detectors ($\sim$8—9 sr c.m.), also triggered on total deposited E_T ("global triggers"), would select hard-scattered events and would allow one to clearly observe the two high-p_T jets.

The first such large-aperture calorimeter data[4] were obtained by the NA5 group at the CERN SPS. Their data showed that, for global triggers, the events were not predominantly of a dijet character, even at the highest E_T observed. Using the variable planarity (P), defined in Ref. 4, to quantify the "jetlikeness" of an event, the NA5 group found $\langle P\rangle \simeq 0.4$ independent of E_T, out to the highest E_T values observed (~ 15 GeV) at $\sqrt{s}=23.8$ GeV. (For well-collimated, back-to-back jets, $P\rightarrow 1$, while for spherically symmetric events $P\rightarrow 0$.) The E557 (Ref. 5), and E609 (Ref. 6) groups found similar results at $\sqrt{s}=27.4$ GeV. Recent ISR (Ref. 7) and pp collider data,[8] however, clearly show that at sufficiently high $\sqrt{s}$ and E_T, a jet signal cleanly emerges even with a global trigger. The interpretation of the lower-energy data ($\sqrt{s}\leq 30$ GeV) remains in question.

The NA5 group carried out a four-jet QCD Monte Carlo simulation based on the Field-Feynman model.[9] Their Monte Carlo results gave $\langle P\rangle \simeq 0.7$ for global triggers with observed $E_T>11$ GeV, rather than 0.40, as seen in the data. The cross sections, $d\sigma/dE_T$, calculated from their Monte Carlo simulation were about an order of magnitude below the data for $E_T>10$ GeV, indicating that a simple four-jet model was inadequate to describe the globally triggered data. The four-jet model was much more successful at reproducing events triggered on smaller solid angles, $\sim$2—4 sr in the c.m.

Other Monte Carlo calculations[10] have invoked gluon bremsstrahlung to account for the lack of apparent dijet structures in globally triggered events. These calculations have been more successful at reproducing planarity distributions and $d\sigma/dE_T$ cross sections, although a recent calculation[5] suggests that planarity distributions for the data and this Monte Carlo disagree for $E_T \gtrsim 14$ GeV. There also has not been agreement about the role of gluon bremsstrahlung. Other authors[11] claim that it is a contributing factor but not nearly sufficient at these energies to account for the large cross sections and low planarities.

Another calculation[12] indicates that a standard four-jet Field-Feynman model reproduces the observed planarity distributions for globally triggered events, in disagreement with the Monte Carlo results of the NA5 group.

This paper presents results from a Field-Feynman four-jet Monte Carlo simulation for high-transverse-energy events at Fermilab/SPS energies. The sensitivity of this calculation to a few features of the model (certainly not all the possible ones) is studied. Somewhat surprisingly, the results are found to be especially sensitive to the method used to ensure overall energy conservation after the fragmentation of the four jets is complete. Parameters which strongly affect the results are the cutoff in the momentum transfer for the QCD subprocesses and the p_T to the jet axis and multiplicities in the fragmentation. Globally triggered events are found to be more sensitive to all of these effects than events triggered on limited solid angles (2—4 sr in the c.m.). With reasonable choices for the features mentioned above, the Monte Carlo results are compared to data from three experiments. The agreement is quite good, certainly comparable to the agreement achieved with a more sophisticated parton-shower model,[10] and in disagreement with the conclusions of Ref. 4. However, with other choices, the Monte Carlo results are qualitatively different and are in strong disagreement with the data.

These results have important implications for extracting physics conclusions from Monte Carlo calculations. It is not possible to distinguish between different models unless they have unambiguous and clearly different predictions. But, as will be demonstrated below, differences in calculational details within one model can lead to very different results. Before one can draw conclusions about the importance of physical processes (such as gluon bremsstrahlung), it is essential to separate effects due to those processes from effects due to differences in details of parton fragmentation or differences in parameters whose values are rather arbitrary.

II. DESCRIPTION OF THE MONTE CARLO CALCULATION

The original version of the program used for this calculation was written by R. A. Singer at Argonne National Laboratory. The structure functions originally suggested by Feynman and Field[9] were used to choose parton types and momenta for input to the hard-scattering process. Only valence quarks and gluons were scattered, no x values below 0.1 were generated, and all partons were taken to be massless. No scale-breaking effects were included in the structure functions. (Scale-breaking effects are expected to be small at these energies.)[13]

Each of the scattered partons was given an intrinsic transverse momentum k_T, such that

$$k_T{}^2 \sim \exp\left[\frac{-k_T{}^2}{2\sigma^2}\right]$$

with $\sigma=0.70$, giving $\langle k_T{}^2\rangle \simeq 1.0\ (\mathrm{GeV}/c)^2$. This value is consistent with results from the Drell-Yan experiments[14] and a previous dijet experiment.[3] The spectator partons balanced the k_T of the scattered partons.

The notation $\hat{s}$, $\hat{t}$, and $\hat{u}$ will be used to represent the Mandelstam variables in the parton-parton center-of-mass frame. For each subprocess, first-order QCD cross sections were used to generate values of $\hat{t}$. Since the QCD cross sections diverge as $\hat{t}\to 0$, it was necessary to impose a cutoff. For most of the work described here, we have used $|\hat{t}| > (1.0\ \mathrm{GeV}/c)^2$. A symmetrical cut was made in the variable $\hat{u}$. The effect of varying this cutoff parameter will be discussed below. The strong coupling constant α_s, was taken to be

$$\alpha_s = \frac{12\pi}{25\ln(Q^2/\lambda^2)} ,$$

with $\lambda^2=0.1\ \mathrm{GeV}^2$ and $Q^2=2\hat{s}\hat{t}\hat{u}/(\hat{s}^2+\hat{t}^2+\hat{u}^2)$.

Fragmentation was done in the c.m. frame of the two scattered partons. One of the spectator quarks (but not gluons) was chosen from the beam and target particles to produce the beam and target jets. Gluons were split into $q\bar{q}$ pairs and each was then fragmented. The parameter a (which determines the probability of a meson in the fragmentation chain carrying a fraction of the remaining parton momentum) was taken to be 0.77, as originally suggested by Feynman and Field. Vector mesons and pseudoscalar mesons were produced with equal probability, and no baryons were produced. The p_T with respect to the jet axis (which will be denoted as q_T) was generated so that

$$q_T{}^2 \sim \exp\left[\frac{-q_T{}^2}{2\sigma^2}\right]$$

with $\sigma=0.35$. This value of σ was chosen (and the distribution was adjusted slightly as a function of parton energy) to achieve good agreement with e^+e^- data.[15,16] Results were found to be quite sensitive to $\langle q_T\rangle$, as will be discussed below.

III. ENERGY AND MOMENTUM CONSERVATION

The question of energy and momentum conservation is difficult. The source of the problem is the fragmentation of *massless* partons into massive particles with momentum components transverse to the parton direction. It is not possible to conserve both energy and momentum in such a fragmentation process. It should be noted that this difficulty is present in *all* models which fragment each parton separately. (Models which use a "string" fragmentation, such as the Lund model,[17] can conserve both energy and momentum in the fragmentation.) I find that (for a single parton) if one requires the longitudinal momentum along the parton direction to be conserved, then the energy is too large: the total energy of all the particles in the jet ($\sum E$) is about 20% larger than the original energy of the parton. If, however, energy is conserved in the fragmentation process, the momentum along the parton direction, summed over all particles in the jet ($\sum p_z$) is only $\sim 80\%$ of the original momentum of the parton. A reasonable compromise is to require

$$\sum(E+p_z)=2p_{\mathrm{parton}} ,$$

where the sum is over all particles in the jet, E is a particle's energy, p_z is a particle's momentum component along the parton direction, and p_{parton} is the momentum of the parton. This is the procedure I have used. However, $\sum E$ is still $\sim 12\%$ greater than the parton energy, and $\sum p_z$ is $\sim 12\%$ smaller than the parton momentum.

Now the question of *overall* energy and momentum conservation arises. The individual momentum components, summed over all particles and calculated in the proton-proton c.m., average to zero with $\sigma = \sim 1$ GeV/c, so that momentum conservation is not violated badly. The total energy in this reference frame (E_{tot}), however, averages to ~ 29 GeV for a true c.m. energy of 27.4 GeV, so that the total energy is overestimated. However, a more subtle effect is at work. Figure 1 shows $\langle E_{\text{tot}} \rangle$ vs E_T observed in a detector which covers $\sim 30° < \theta_{\text{c.m.}} < 130°$, a typical global trigger. One sees that the average total energy increases with E_T so that at the highest E_T, the total energy is overestimated by $\sim 20\%$. (Here we are not considering the effects of detector energy resolution. The conclusions reached below are not changed if the total E_T in the event is considered, rather than E_T into a particular solid angle.)

The origin of this effect becomes clear when one studies event structure as a function of observed E_T. Figure 2 shows that the average charged multiplicity $\langle n_{\text{ch}} \rangle$ increases from ~ 16 at $E_T = 6$ GeV to ~ 24 at $E_T = 15$ GeV, an increase of $\sim 50\%$. The average p_T to the jet axis $\langle q_T \rangle$ also increases by $\sim 15\%$ over this region for the beam jet, from 0.35 GeV/c at $E_T = 6$ GeV to 0.4 GeV/c at $E_T = 15$ GeV. The $\langle q_T \rangle$ for the scattered jets is also $\sim 15\%$ larger for these high-E_T events than for untriggered events. Both of these effects contribute to the overestimation of the total energy. It is clear that a global E_T trigger selects events which have obtained large E_T at least in part by having fragmentation modes with larger-than-average multiplicities and larger-than-average momentum components transverse to the jet direction.

Now the question becomes how to impose energy and momentum conservation. I will discuss one method of momentum conservation and two methods of energy conservation and how they affect event structure (these are certainly not the only possible choices).

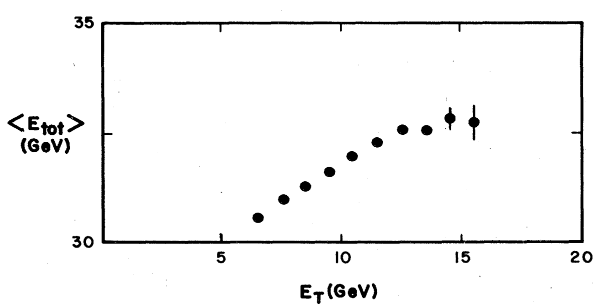

FIG. 1. Average center-of-mass energy before applying energy conservation versus E_T observed in a detector covering $30° \leq \theta_{\text{c.m.}} \leq 130°$. The correct center-of-mass energy is 27.4 GeV.

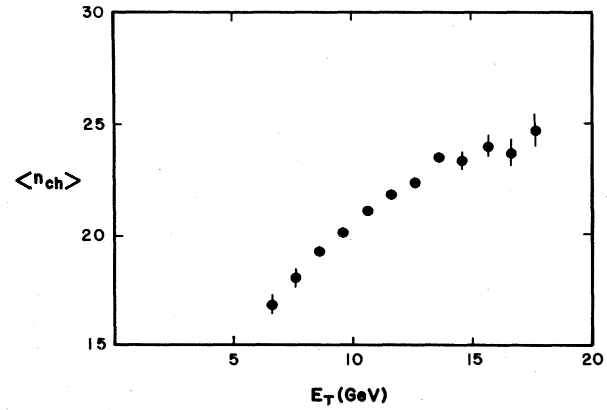

FIG. 2. Average value of charged multiplicity versus E_T. No overall energy conservation has been applied.

Momentum conservation does not present a problem since the original deviation from conservation is small. One simple method, carried out in the proton-proton c.m., is an averaging technique. The sums $\sum p_i$ are formed for each momentum component, where the sum is over all particles in the event. Then $\sum p_i / n$ is subtracted from each particle's momentum component, where n is the total multiplicity, thus ensuring exact momentum conservation. These corrections to the momentum components were on the average ~ 5 MeV/c and have little effect on event structure.

Energy conservation, however, is more difficult since $\delta E / E$ is fairly large and E_T dependent. Two methods of imposing energy conservation are described below.

(1) All momentum components of all particles are multiplied by a scale factor, determined iteratively, such that the total energy is within some tolerance (0.1% was used for our calculations) of the correct value. This procedure was carried out in the overall c.m. so that momentum conservation was unaffected. This procedure does change laboratory angles of particles slightly, since $\theta_{\text{c.m.}}$ is unchanged but particle energy is decreased. The planarity of the event is not affected, but the observed E_T *does* change, in some cases by several GeV.

(2) Only momentum components *parallel* to the beam are scaled down, again by a factor determined iteratively, to achieve the correct energy. This procedure also changes laboratory angles of particles but preserves the total E_T of the event. Planarity of the event is also unaffected, since it depends only on the transverse momentum components. However, variables which depend on all three momentum components, such as sphericity or thrust, will be affected by this procedure. Also, E_T into a given solid angle can be changed due to the change in particle laboratory angle, but this change is at most 1 GeV.

Both of these methods of imposing energy conservation have a slight effect on jet structure. I have checked that the multiplicities and *final* jet structure for triggered events agree well with e^+e^- jets by transforming the final-state particles back to the parton-parton c.m. and recalculating q_T and rapidity along the jet axis (y). The parameters of the fragmentation were adjusted slightly so that distributions of q_T and y for method (2) agrees well (within $\sim 5\%$) with e^+e^- data.[15,16] This same set of parameters leaves $\langle q_T \rangle \sim 10\%$ too small for method (1). However, changing the parameters so that $\langle q_T \rangle$ is correct for method (1) does not qualitatively change the conclusions to be discussed below.

Imposing energy conservation by method (1) might seem like the most natural choice. But it has a curious effect. Since for global triggers the average total energy increases with E_T, the scale factor used to correct the momentum components to achieve the correct energy *decreases* with E_T. If the transverse components as well as the longitudinal components are scaled down, E_T is lost in the process, and nearly every large-E_T event is simply scaled back down to low or intermediate E_T. To demonstrate this effect, Fig. 3(a) shows the change in E_T (ΔE_T) introduced by imposing energy conservation for both methods for global E_T triggers at $\sqrt{s}=27.4$ GeV. Negative values of ΔE_T indicate that E_T has been lost in the process. Using method (1), the larger the *original* E_T, the larger the E_T lost in the energy conservation process. However, method (2), by definition, preserves the original total E_T.

The effect of method (1) is slightly more complicated. At a given original E_T, low-planarity events tend to have larger multiplicity and q_T values than high-planarity events, leading to larger overestimates of the total energy. So with method (1), the change in E_T introduced by the energy-conservation procedure is greater for low-planarity events than for high-planarity events. Low-planarity events are moved down to a lower final E_T, whereas high-planarity events remain closer to their original E_T value. For example, for $11 < E_T < 12$ GeV and $P \leq 0.1$, the average change in E_T is -2.5 GeV while for $P \geq 0.9$, the average ΔE_T is -1.2 GeV.

The net result is that for globally triggered events method (1) tends to bias against events at high E_T which obtained a large fraction of the final E_T from the fragmentation. Those events are still produced, they are simply moved down to lower E_T values. This effect is clearly seen by comparing $\langle n_{\rm ch} \rangle$ versus final E_T for the two methods of energy conservation, as shown in Fig. 3(b). For method (2), $\langle n_{\rm ch} \rangle$ increases with E_T, as observed earlier, but for method (1), $\langle n_{\rm ch} \rangle$ actually flattens off and may decrease for $E_T \gtrsim 11$ GeV. The values of $\langle q_T \rangle$ are also somewhat different: for method (1), $\langle q_T \rangle$ is ~ 0.33 GeV/c at $E_T = 6$ GeV and increases $\sim 6\%$ up to $E_T \sim 15$ GeV, while for method (2), $\langle q_T \rangle$ is ~ 0.35 at $E_T = 6$ GeV and increases $\sim 15\%$ out to E_T of ~ 15 GeV.

Since method (1) biases against obtaining substantial E_T from the fragmentation, it follows that high-E_T events generated in this way must obtain more of their E_T from the hard scatter. Figure 3(c) compares the distributions for p_T of the hard scatter for final E_T in the region $30° \leq \theta_{\rm c.m.} \leq 130°$ greater than 11 GeV. For method (1), the p_T peaks at ~ 5 GeV/c, indicating a fairly hard scatter on the parton level. For method (2), p_T is sharply peaked at the cutoff value of 1 GeV/c, indicating that the scatters on the parton level are quite soft, with most of the E_T in the detector arising from the fragmentation. In particular, on the average only half of the detected E_T

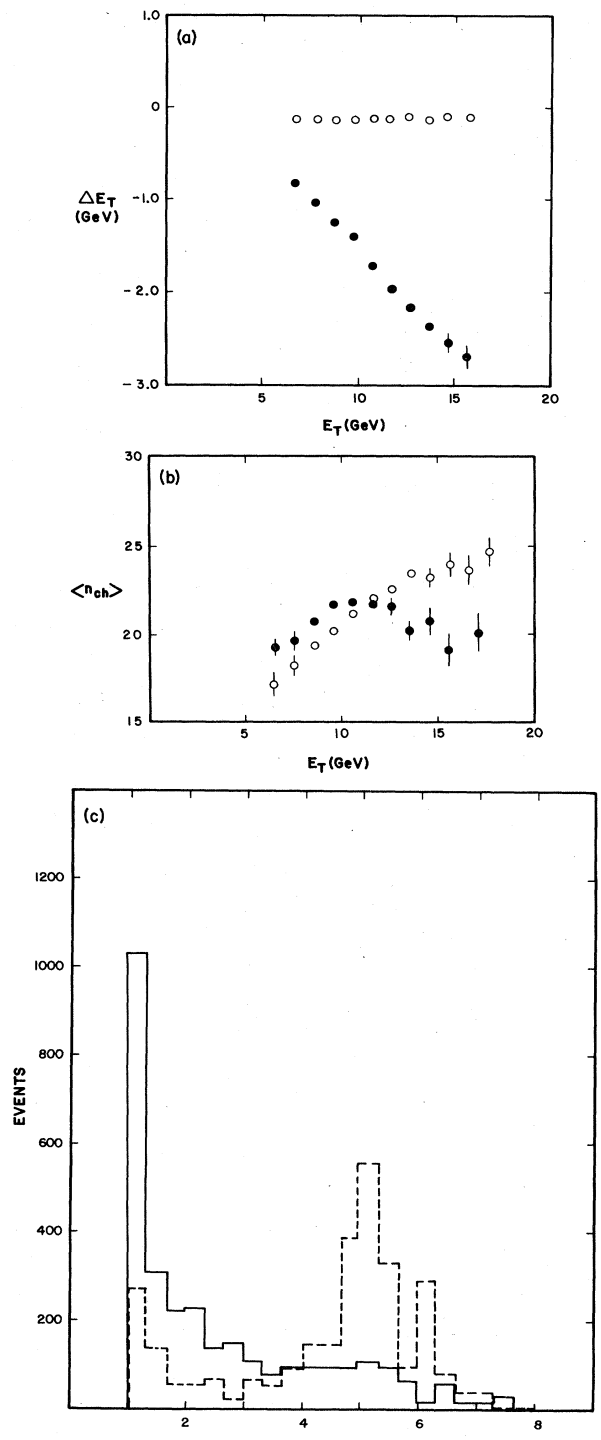

FIG. 3. Comparison of the effects of the two methods of energy conservation (as described in the text) on event structure. The solid points in (a) and (b) and dashed line in (c) refer to method (1), and the open points in (a) and (b) and solid curve in (c) refer to method (2). (a) Change in E_T as a result of energy conservation versus original E_T. The change in E_T is calculated for particles with original angles in the range $30° < \theta_{\rm c.m.} < 130°$. (b) Average charged multiplicity versus final E_T. (c) p_T in the hard-scattering process for final $E_T > 11$ GeV. In all cases, E_T values used are for particles in the range $30° \lesssim \theta_{\rm c.m.} \lesssim 130°$.

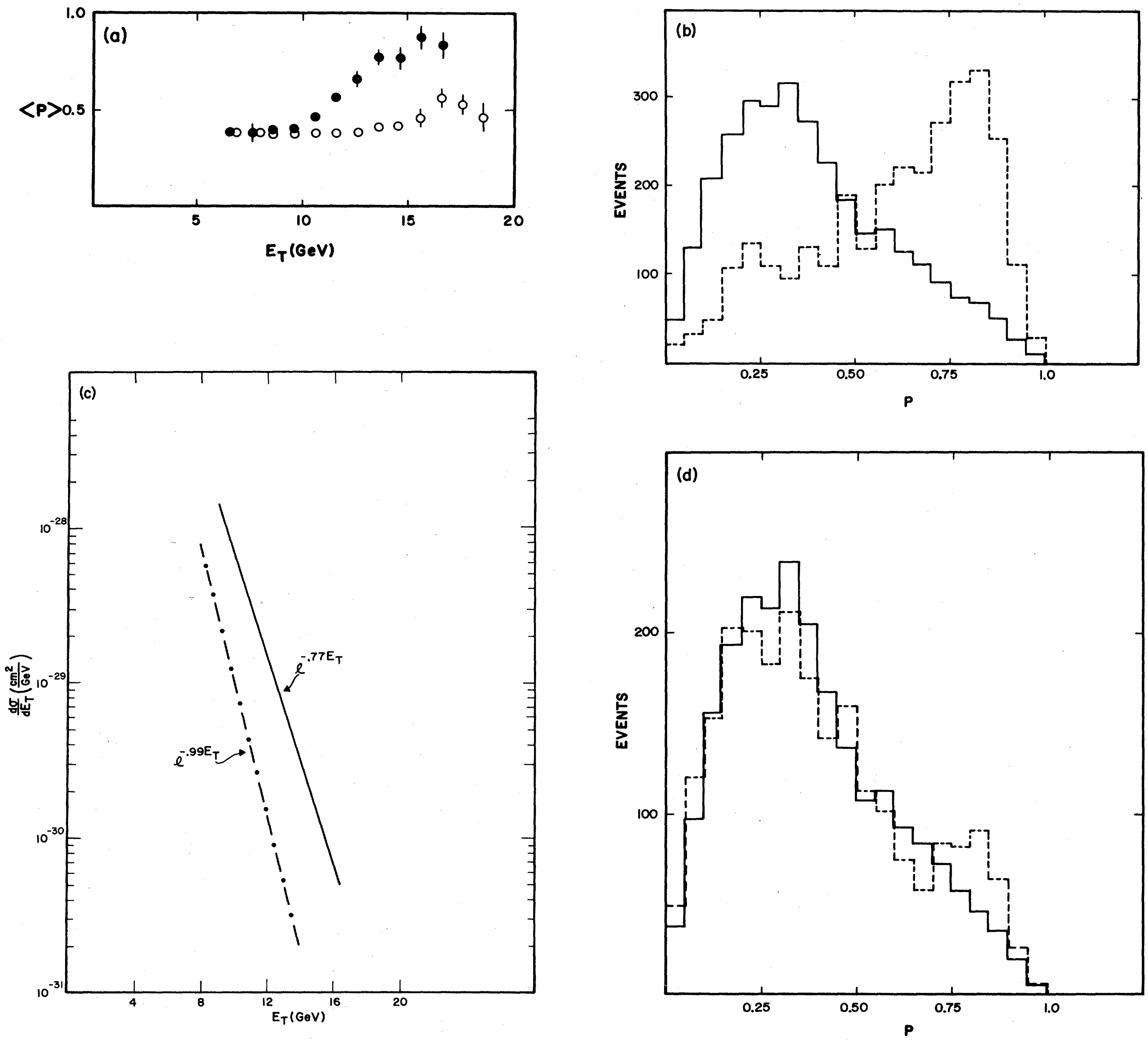

FIG. 4. Comparison of Monte Carlo results for the two methods of energy conservation. (a) Average planarity versus final E_T. The solid points refer to method (1), as described in the text, and the open points refer to method (2). (b) Normalized planarity distributions for $E_T > 11$ GeV. The dashed curve refers to method (1) and the solid curve to method (2). (c) Cross section $d\sigma/dE_T$ versus E_T. The dotted-dashed curve refers to method (1) and the solid curve to method (2). (d) Comparison of planarity distributions for $E_T > 11$ GeV for different fragmentation procedures. The solid curve results when $(E+p_z)$ is conserved in the fragmentation, and the dashed curve corresponds to conserving E in the fragmentation. In all cases, the E_T values used are those observed in the range $30° \leq \theta_{\text{c.m.}} \lesssim 130°$.

comes from the scattered partons, with the other half coming from the beam and target jets.

Figure 4 shows how radically the two methods of energy conservation differ in final event structure for global triggers. It should be emphasized that the *only* difference between the results shown here is the method used to ensure overall energy conservation after the fragmentation of the four jets. Figure 4(a) compares $\langle P \rangle$ vs E_T for particles into $30° < \theta_{\text{c.m.}} < 130°$ at $\sqrt{s} = 27.4$ GeV. For method (1), $\langle P \rangle$ begins to increase at $E_T = 10$ GeV, while for method (2), $\langle P \rangle$ is flat out to 15 GeV, after which it may be increasing. Figure 4(b) compares planarity distributions for $E_T > 11$ GeV, and Fig. 4(c) compares the cross section $d\sigma/dE_T$. The planarity distributions are radically different and the cross sections differ by about an order of magnitude above $E_T \sim 10$ GeV. It should be noted that the results of method (2) are the same as if no energy conservation had been applied, since method (2) does not change either P or total E_T and increases E_T by 1 GeV or less in the triggering region. It is clear from these results that details of the fragmentation procedure and questions of energy and momentum conservation are critical to any conclusions about the predictions of this or similar Monte Carlo calculations.

The striking difference between these two methods of energy conservation arises only because an E_T trigger is imposed on the events. The Monte Carlo (like nature) will provide the E_T in the most economical way. Any step in the fragmentation procedure which reduces the final E_T will have a profound effect on the event sample which passes the trigger. Events which have not been triggered on E_T do not show such a startling difference between the two methods of energy conservation.

Another approach to the problem of overall energy conservation is simply to choose to conserve energy in the fragmentation chain rather than $(E+p_z)$. Then the total energy after fragmentation is exactly correct, and only small changes must be made to conserve momentum exactly. However, this choice is actually nearly equivalent to method (2) above, since in both cases energy is conserved for the most part at the expense of the momentum components longitudinal to the parton direction. Figure 4(d) compares planarity distributions for $E_T > 11$ GeV obtained by conserving E in the fragmentation to those obtained by method (2). The distributions are in good agreement.

IV. LIMITED-SOLID-ANGLE TRIGGERS

The problem of energy and momentum conservation becomes much less severe when one triggers on E_T in a smaller solid-angle region, about 2—4 sr in the c.m. rather than 8—9 sr. Such a trigger will be less sensitive to high-multiplicity fragmentation modes of both the beam and target remnants and the scattered partons. And for that reason smaller solid-angle triggers will also be much less sensitive to the method used to conserve energy.

Figure 5 shows the results from a "double-arm" trigger consisting of two coplanar regions, each ~ 2 sr in the c.m. and each at $\theta_{\mathrm{c.m.}} \simeq 80°$. Figure 5(a) shows $\langle P \rangle$ vs E_T in the triggering region and 5(b) shows the planarity distribution for $E_T > 9$ GeV in the triggering region. The two methods of energy conservation described in Sec. III are compared. Method 1 still gives a more planar-event structure, but the difference is not nearly as striking as for global triggers. Both methods now show a rise in $\langle P \rangle$ with increasing E_T, although method 1 shows the rise at lower E_T. The cross sections $d\sigma/dE_T$ differ in this case by about a factor of 4, rather than an order of magnitude as was the case for global triggers.

The rise in $\langle P \rangle$ with increasing E_T deserves some comment. In this model, when a high-E_T trigger is imposed, there is a competition between obtaining the E_T from high-multiplicity fragmentation modes of the partons and obtaining it from the hard scatter. As the E_T threshold is increased, it becomes more difficult to supply the E_T from the fragmentation. The soft contribution therefore decreases and the hard contribution increases with increasing E_T. The rise in $\langle P \rangle$ indicates the point at which the hard scattering begins to dominate. The smaller the

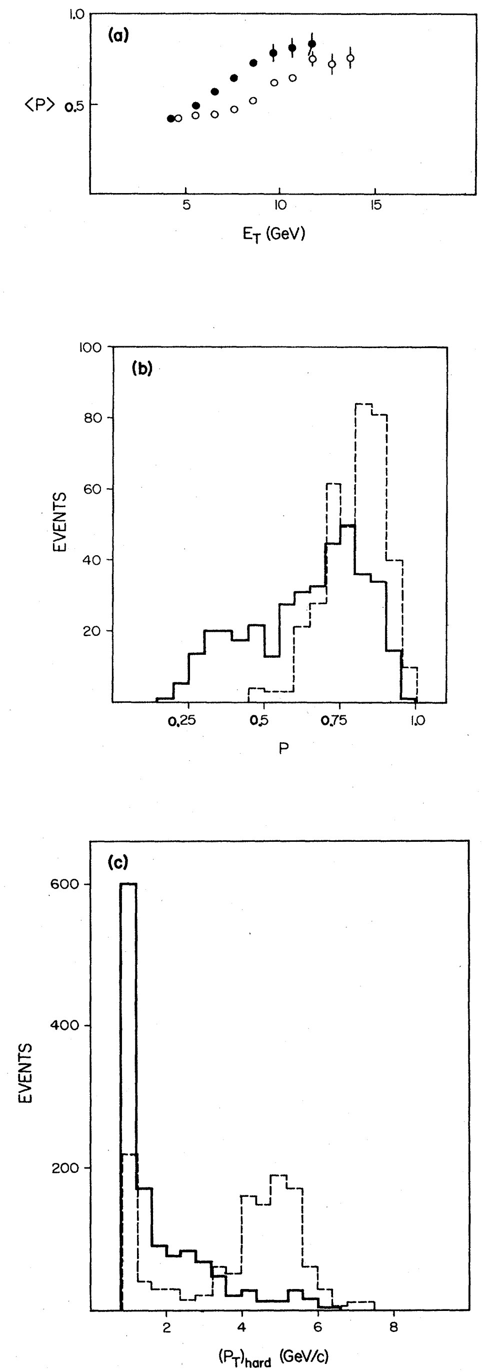

FIG. 5. Monte Carlo results for a double-arm trigger of two coplanar regions, each of 2 sr solid angle in the c.m. and $\theta_{\mathrm{c.m.}} \simeq 80°$. In all cases the E_T is E_T in the trigger region. (a) $\langle P \rangle$ vs E_T, comparing the two methods of energy conservation as described in the text. The solid points are method (1); the open points are method (2). (b) Normalized planarity distributions for $E_T > 9$ GeV. The dashed curve is method (1); the solid curve is method (2). (c) Distribution in p_T of the hard scatter for two E_T cuts using method (2) for energy conservation. The solid curve is for $E_T > 6$ GeV, and the dashed curve is for $E_T > 9$ GeV.

solid angle of the trigger, the sooner this crossover occurs, as can be seen by comparing $\langle P \rangle$ vs E_T for the double arm and global triggers. This dependence on solid angle has been observed before.[18] It is also clear that energy-conservation method (1) causes the crossover to occur at lower values of E_T than method (2). The reason is clear—as mentioned before, method 1 biases against obtaining a large part of the E_T from the fragmentation.

Figure 5(c) compares the distributions of p_T of the hard scatter for E_T in the double-arm trigger region greater than 6 GeV and greater than 9 GeV, using method 2 for energy conservation. For the higher E_T, the emergence of the hard-scattering signal is evident. $E_T \simeq 9$ GeV is also the region where $\langle P \rangle$ begins to increase for this trigger. The emergence of the hard-scattering signal has also been seen using the QCD cluster Monte Carlo simulation of Ref. 10 for the "two-high" trigger used by the E609 collaboration.[19] (The two-high trigger requires any two towers of the calorimeter to have E_T above a threshold of ~ 1 GeV.)

The data at Fermilab/SPS energies do exhibit such a rise in $\langle P \rangle$ vs E_T for triggers of $\sim$2–4 sr solid angle, as will be shown in Sec. VI. However, $\langle P \rangle$ for global triggers does not rise even for the largest E_T's observed, which are in the range of 15—20 GeV. At ISR energies,[7] $\langle P \rangle$ is seen to rise for global triggers for $E_T \sim 30$ GeV, which has been interpreted as the emergence of a jet signal.

A "single-arm" trigger (for example, just one section of the calorimeter with solid angle ~ 2 sr in the c.m. and $\theta_{\mathrm{c.m.}} \simeq 80°$) behaves similarly to the double-arm trigger described above. $\langle P \rangle$ begins to increase at even lower values of E_T in the trigger region, and the differences between the two methods of energy conservation are even less.

V. EFFECTS OF OTHER PARAMETERS

For the effects discussed in this section, method 2 has been used for the energy conservation. Quantitative Monte Carlo results for globally triggered events are quite sensitive to both average multiplicity and q_T. As an example, allowing the beam and target jets to be gluons, a fraction of the time appropriate for the structure functions, increases the multiplicity by $\sim 5\%$ and increases $\langle q_T \rangle$ by a similar amount. These changes together increase $d\sigma/dE_T$ about a factor of 2. A change of $\sim 10\%$ in $\langle q_T \rangle$ alone has about the same effect. Such sensitivity to the fragmentation parameters indicates that quantitative cross sections should not be taken seriously to at least a factor of 2. Limited-solid-angle triggers are less sensitive to this effect, with $d\sigma/dE_T$ increasing only $\sim 25\%$ when $\langle q_T \rangle$ is increased by 10% for the double-arm trigger described in the previous section.

Results from the Monte Carlo simulation for global triggers are also sensitive to the minimum value of $|\hat{t}|$ ($|\hat{t}|_{\min}$) generated. Figure 6 shows planarity distributions for $E_T > 11$ GeV for $|\hat{t}| > 1.0$ (GeV/c)^2 and $|\hat{t}| > 10.0$ (GeV/c)^2. These limits on $\hat{t}$ correspond to p_T of the hard scatter greater than 1 GeV/c and ~ 2.5 GeV/c, respectively. As would be expected, a higher $|\hat{t}|_{\min}$ gives a much more planar-event structure. Cross sections are also strongly affected by the $|\hat{t}|$ cutoff, as is clear from Fig. 3(c). Even for $E_T > 11$ GeV (for method 2), most of the events arise from $\hat{t}$ values near the cutoff. Changing the cutoff from 1.0 to 2.0 (GeV/c)^2 decreases $d\sigma/dE_T$ about a factor of 3 for E_T from 10 to 15 GeV.

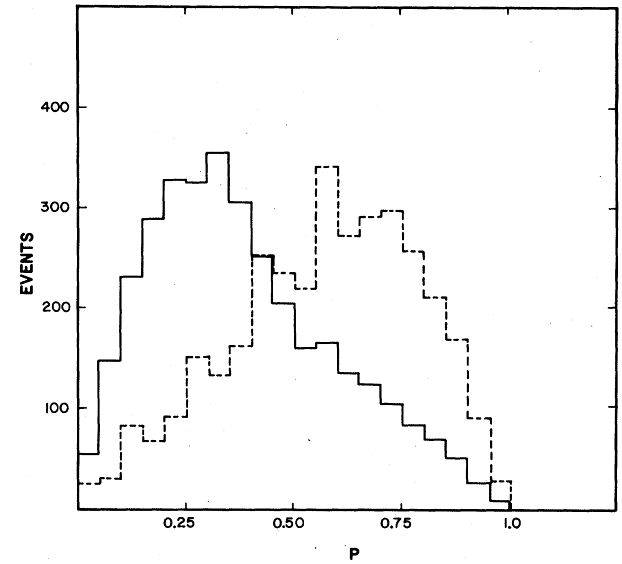

FIG. 6. Normalized planarity distributions for $E_T > 11$ GeV for $|\hat{t}| > 1.0$ (GeV/c)^2 (solid curve) and $|\hat{t}| > 10.0$ (GeV/c)^2 (dashed curve). These cutoffs in $\hat{t}$ correspond to cutoffs in p_T of the hard scatter of 1.0 GeV/c and ~ 2.5 GeV/c, respectively.

Below the E_T value at which $\langle P \rangle$ rises, the double-arm triggers are also sensitive to the cutoff in $|\hat{t}|$. But in the region where $\langle P \rangle$ has increased to ~ 0.6 or above ($E_T \gtrsim 9$ GeV), the double-arm triggers are much less sensitive to this cutoff, as can be seen clearly in Fig. 5(c). For $E_T > 9$ GeV, scatters on the parton level of $p_T \lesssim 2$ GeV/c do not easily satisfy the trigger, and their contribution decreases with increasing E_T. As long as $|\hat{t}|_{\min}$ in the Monte Carlo is below the effective cutoff imposed by the trigger, the Monte Carlo results are not sensitive to $|\hat{t}|_{\min}$. The same comments apply to the single-arm and two-high triggers. Global triggers, on the other hand, are sensitive to soft scatters on the parton level out to E_T values of at least 15 GeV.

VI. COMPARISON WITH DATA

As discussed earlier, three different experiments at Fermilab energies have obtained data using a large-solid-angle calorimeter, and all agree well on the general features of the data (although perhaps not on magnitudes of cross sections).

For comparison to the data, only true particle momenta have been used, without taking into account energy resolution effects of various detectors. Method 2 has been used for energy conservation in all cases. It should be kept in mind that experimental E_T scales are uncertain to 5—10%.

Figure 7 compares the Monte Carlo with NA5 data at $\sqrt{s} = 23.8$ GeV. Figure 7(a) compares $\langle P \rangle$ vs E_T for

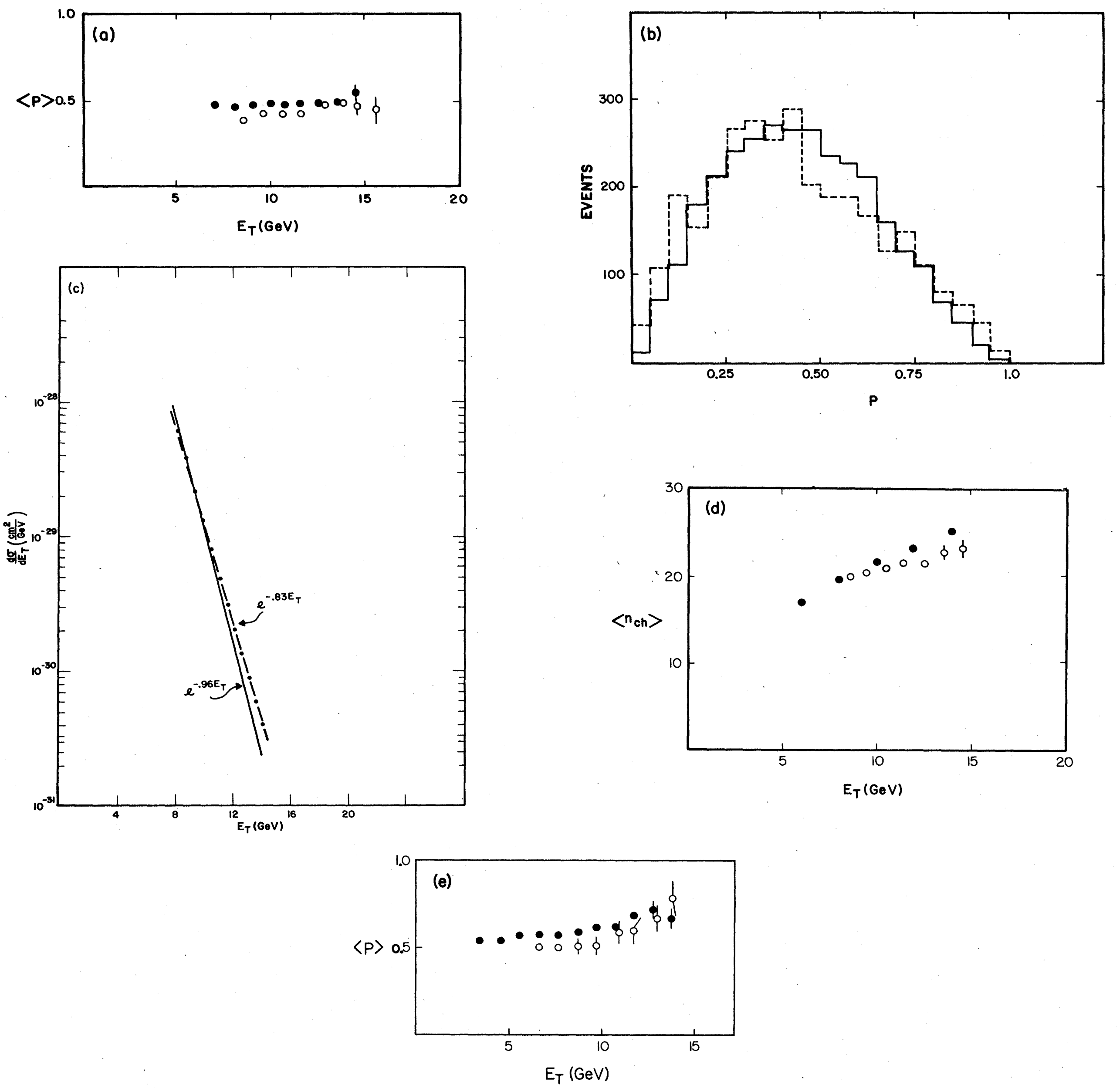

FIG. 7. Comparison of Monte Carlo results with NA5 data. (a) $\langle P \rangle$ vs E_T, πp interactions for the data (solid points) and pp interactions for the Monte Carlo simulation (open points) for the global trigger. (b) Planarity distributions for $E_T > 11$ GeV for pp interactions for the global trigger. The solid curve is NA5 data, the dashed curve is the Monte Carlo simulation. (c) Cross section $d\sigma/dE_T$ vs E_T for the global trigger. The solid curve is the data, the dotted-dashed curve is the Monte Carlo. (d) Total average charged multiplicity vs E_T. The solid points are data; the open points are from the Monte Carlo simulation. (e) $\langle P \rangle$ vs E_T for a double-arm trigger of two coplanar regions, each of solid angle 2.7 sr in the c.m. and $\theta \simeq 90°$. The solid points are NA5 data; the open points are from the Monte Carlo simulation.

data with an incident *pion* beam and Monte Carlo with an incident *proton* beam for a global trigger, with E_T in the region $54° < \theta_{\text{c.m.}} < 135°$. (The experimenters did not report a result for $\langle P \rangle$ vs E_T for the pp data, although they state that the πp and pp results are similar. P is slightly higher for πp interactions, however.) $\langle P \rangle$ for the Monte Carlo results is slightly lower than the data, and both are flat out to the highest E_T values reached. Figure 7(b) compares planarity distributions for $E_T > 11$ GeV for pp interactions for the global trigger, and Fig. 7(c) compares the global cross sections $d\sigma/dE_T$. Agreement is excellent for both. Figure 7(d) compares average total charged multiplicity vs E_T and again, agreement is quite good, although the Monte Carlo is slightly below the data. Figure 7(e) shows good agreement between data and Monte Carlo for a double-arm trigger of solid angle 2×2.7 sr centered

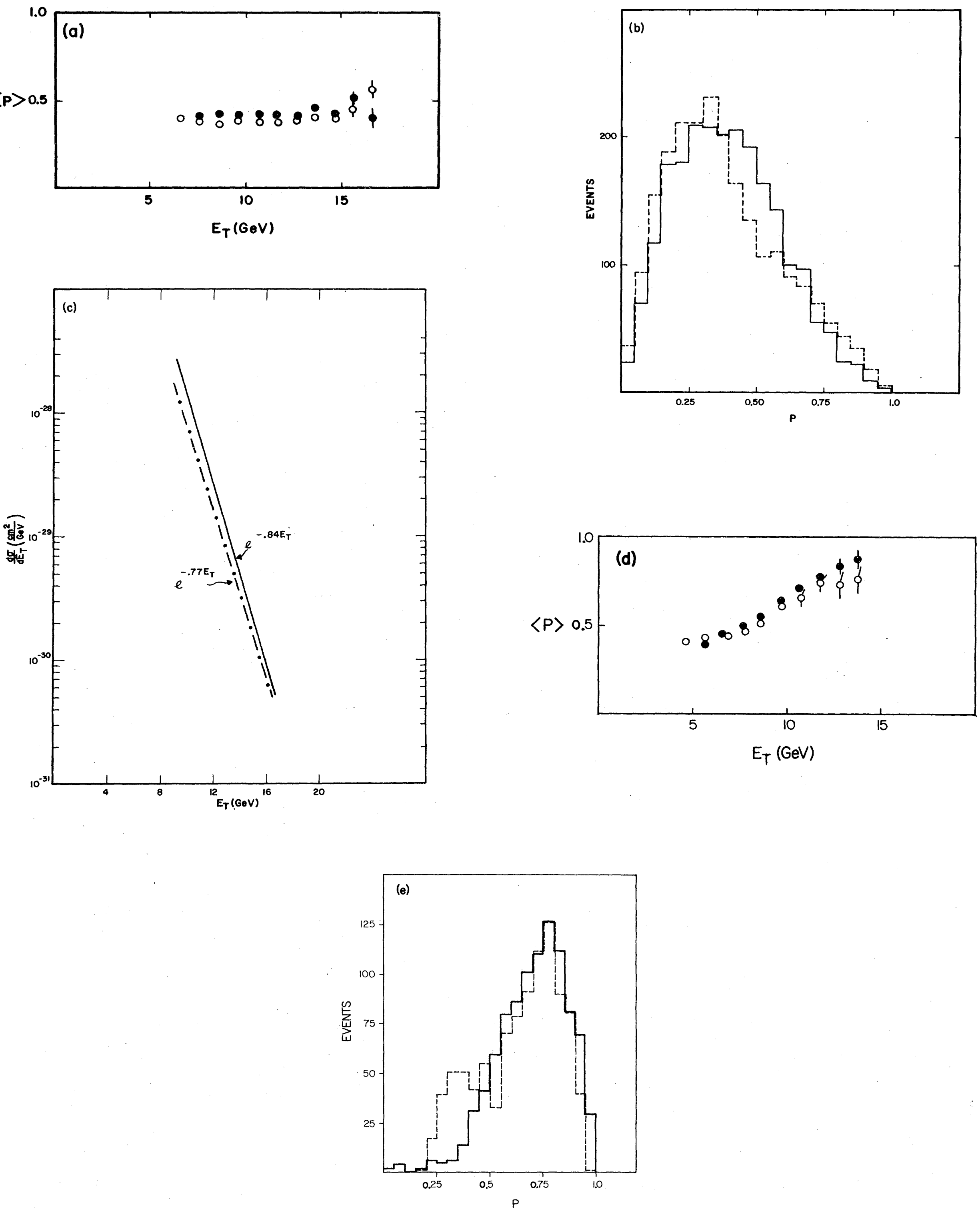

FIG. 8. Comparison of Monte Carlo and E609 data. Notation for data and Monte Carlo simulation is the same as Fig. 7. (a) $\langle P \rangle$ vs E_T for a global trigger. (b) Planarity distributions for $E_T > 11$ GeV for a global trigger. (c) Cross sections $d\sigma/dE_T$ vs E_T for a global trigger. (d) $\langle P \rangle$ vs E_T for a double-arm trigger of two coplanar sections of the calorimeter, each of solid angle ~ 2 sr and $\theta_{c.m.} \simeq 80°$. (e) Planarity distributions for $E_T > 9$ GeV for the double-arm trigger.

at $\theta_{\text{c.m.}} = 90°$.

These results for the global trigger are in strong disagreement with the four-jet Monte Carlo results reported by the NA5 collaboration.[4] Although it is not stated in their papers, it seems likely that they used an energy-conservation method similar or identical to method (1) described above. As shown in Fig. 4, for global triggers method (1) gives a much more planar-event structure and a cross section lower by an order of magnitude than method (2). These are exactly the Monte Carlo results reported by the NA5 group. Another important difference is that the NA5 Monte Carlo used only events with p_T of the hard scatter $\gtrsim 2.5$ GeV/c. As shown by the dashed curve in Fig. 6, this higher cutoff results in a much more planar-event structure, and it certainly affects the global cross section. It is interesting to note that, as shown by the dashed curve in Fig. 3(c), a cutoff of 2.5 GeV/c in p_T of the hard scatter would seem quite reasonable if energy conservation method (1) were used.

The NA5 group found better agreement between the Monte Carlo simulation and their limited-solid-angle data, in agreement with the conclusions of Sec. IV. The limited-solid-angle triggers are less sensitive to the problems of energy and momentum conservation and the $|\hat{t}|$ cutoff.

Figure 8 compares the Monte Carlo with E609 data for pp interactions at $\sqrt{s} = 27.4$ GeV. Figure 8(a) compares $\langle P \rangle$ vs E_T, Fig. 8(b) compares planarity distributions for $E_T > 11$ GeV, and Fig. 8(c) compares $d\sigma/dE_T$, all for a global trigger with E_T in the region $30° \lesssim \theta_{\text{c.m.}} \lesssim 130°$. Agreement is good in all cases, although the planarity distribution [Fig. 8(b)] is slightly softer for the Monte Carlo than for the data. Figure 8(d) compares $\langle P \rangle$ vs E_T for a double-arm trigger of $\sim 2 \times 2$ sr solid angle at $\theta_{\text{c.m.}} \simeq 80°$, and Fig. 8(e) compares the planarity distributions for $E_T > 9$ GeV in the trigger region. Agreement is good, although again the planarity distribution is slightly softer for the Monte Carlo than for the data.

Figure 9 compares the Monte Carlo with E557 data at $\sqrt{s} = 27.4$ GeV. Figures 9(a), 9(b), and 9(c) are all for a

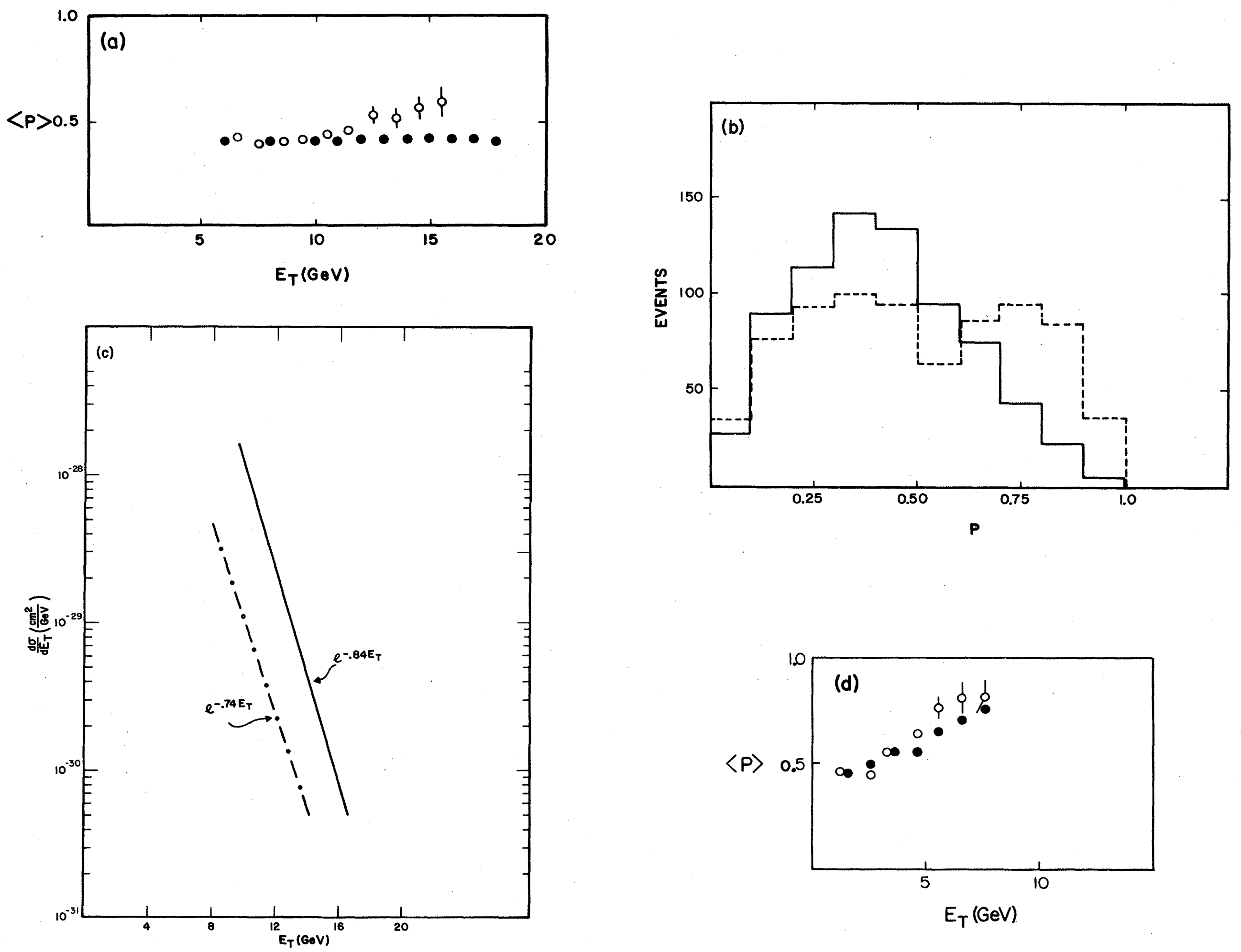

FIG. 9. Comparison of Monte Carlo and E557 data. Notation for data and Monte Carlo simulation is the same as Fig. 7. (a) $\langle P \rangle$ vs E_T for a global trigger. (b) Planarity distributions for $E_T > 15$ GeV for the data and $E_T > 11$ GeV for the Monte Carlo for a global trigger. (c) Cross sections $d\sigma/dE_T$ vs E_T for a global trigger. (d) $\langle P \rangle$ vs E_T for a single-arm trigger of solid angle ~ 1 sr and $\theta_{\text{c.m.}} \simeq 90°$.

global trigger with $47° < \theta_{\text{c.m.}} < 127°$. Figure 9(a) shows $\langle P \rangle$ vs E_T; the data are flat out to the highest E_T values reached, while the Monte Carlo indicates a rise with E_T. Figure 9(b) shows planarity distributions for the data with $E_T > 15$ GeV and the Monte Carlo for $E_T > 11$ GeV. The Monte Carlo distribution has an excess of events at high planarity compared to the data, although the agreement is not too bad. Figure 9(c) compares the cross sections. The Monte Carlo falls about an order of magnitude below the E557 data. This discrepancy in the magnitude of the cross section has been noticed before with a model which includes gluon bremsstrahlung.[10] Overall, the agreement with the E557 global data is not nearly as good as the agreement with the other two experiments. Figure 9(d) shows $\langle P \rangle$ vs E_T for a single-arm trigger of solid angle 1 sr and $\theta_{\text{c.m.}} = 90°$, and in this case agreement is quite good.

This lack of agreement for the global data requires further comment. First of all, there seems to be a real discrepancy in the absolute magnitudes of the cross sections between the E557 and E609 results. As can be seen from Figs. 8(c) and 9(c), the measured cross sections are nearly identical, but they should *not* be, since the acceptance of the E557 detector is considerably smaller than the E609 detector. However, both experiments report an uncertainty in the E_T scale of 5—7 %.

The rise seen in the Monte Carlo for $\langle P \rangle$ at high E_T [Fig. 9(a)] is due to the emerging dominance of the hard scattering, as discussed in Sec. IV. It is seen for the Monte Carlo results in Fig. 9(a) and not in Fig. 8(a) because the solid angle of the E557 detector is somewhat smaller than that of E609.

As mentioned before, the ISR data[7] indicate that with a global trigger, P begins to increase at $E_T \simeq 30$ GeV for $\sqrt{s} = 45$ and 63 GeV. It would appear that this Monte Carlo gives the rise in P for global triggers at a value of E_T somewhat too low. This situation could be remedied, at least in part, by allowing $\langle q_T \rangle$ to increase with parton energy, as indicated by e^+e^- data at higher energies.[15,16]

VII. CONCLUSIONS

A four-jet Field-Feynman Monte Carlo simulation has been used to study the production of high-E_T events at Fermilab/SPS energies. The results are found to be especially sensitive to the method used to assure overall energy conservation after the fragmentation is complete, and a global trigger is found to be especially sensitive to this problem. In particular, a method of energy conservation which changes the observed E_T changes in a drastic way both the event structure for the events which pass the global E_T trigger and also the observed cross sections $d\sigma/dE_T$. The model also exhibits sensitivity to the cutoff in $\hat{t}$ of the QCD subprocesses and to the multiplicities and the distribution in q_T in the parton fragmentation. The global trigger is more sensitive to all of these features than events triggered on smaller solid angles of $\sim$2—4 sr in the c.m. With an energy-conservation method which does not change the observed E_T, and with reasonable choices of the other features mentioned above, a four-jet Field-Feynman Monte Carlo simulation gives a good description of the main features of the experimental data. This is in agreement with Ref. 11 and in disagreement with the conclusions of Ref. 4. It seems likely that the discrepancy between these results and those of Ref. 4 is due to different methods of imposing overall energy conservation and different cutoff values of $\hat{t}$.

Other methods of energy conservation besides the ones mentioned here are certainly possible, and other methods may introduce other types of biases. The problem of energy conservation arises in all independent fragmentation models of this type. Because the E_T spectrum falls steeply, it is not surprising that changing the observed E_T, when one is requiring high E_T, has a drastic effect on the results. It would seem preferable in this case to choose a method which does not make large changes in the observed E_T "after the fact." Even more preferable would be a fragmentation scheme which conserves energy and momentum from the outset, so that this problem does not arise.

The agreement between the data and this calculation is comparable to the agreement achieved by the QCD-motivated parton-shower model of Ref. 10. (The model of Ref. 10, incidently, does not conserve energy event-by-event, but only on the average.)[20] Differences between the simple four-jet model described here and more sophisticated ones are of interest in order to understand the fundamental QCD processes involved. However, before one can validly draw conclusions about the physics, it is necessary to show that different models have clearly different predictions which do not depend sensitively on rather arbitrary details of the calculation.

ACKNOWLEDGMENTS

It is a pleasure to acknowledge the many useful discussions with all my colleagues in the E609 collaboration, in particular, Tom Fields, Walter Selove, Ken Johns, Chuck Naudet, Hannu Miettinen, G. C. Phillips, and Al Erwin. I also gratefully acknowledge the work of Rich Singer in writing the original version of the Monte Carlo. Students who have helped with the programming and other calculations include Jim Flowers, Craig Hansen, Gordon Carrie, and Roxanne Springer. This work was supported by the U. S. Department of Energy.

[1] *Proceedings of the Symposium on Jets in High Energy Collisions, Copenhagen, 1978* [Phys. Scr. **19**, 1 (1979)].

[2] C. Bromberg *et al.*, Phys. Rev. Lett. **38**, 1447 (1977); Nucl. Phys. **B134**, 189 (1978).

[3] M. D. Corcoran *et al.*, Phys. Rev. Lett. **41**, 9 (1978); **44**, 514 (1980); Phys. Rev. D **21**, 641 (1980).

[4] C. deMarzo *et al.*, Phys. Lett. **112B**, 173 (1982); Nucl. Phys. **B211**, 375 (1983); **B234**, 1 (1984).

[5] B. Brown *et al.*, Phys. Rev. Lett. **49**, 711 (1982); Phys. Rev. D **29**, 1895 (1984).

[6] W. Selove *et al.*, in *Proceedings of the 21st International Conference on High Energy Physics, Paris, 1982*, edited by P. Petiau and M. Porneuf [J. Phys. (Paris) Colloq. **43**, C3-131, 1982]; M. A. Arenton *et al.*, Report No. ANL-HEP-PR-83-

26 (unpublished); M. A. Arenton *et al.*, Phys. Rev. D **31**, 984 (1985).

[7]A. L. S. Angelis *et al.*, Phys. Lett. **105B**, 233 (1981); T. Åkesson *et al.*, Phys. Lett. **118B**, 185 (1982); **118B**, 193 (1982); **128B**, 354 (1983).

[8]G. Arnison *et al.*, Phys. Lett. **118B**, 173 (1982); M. Banner *et al.*, *ibid.* **118B**, 203 (1982); G. Arnison *et al.*, *ibid.* **132B**, 214 (1983); G. Sauvage *et al.*, Report No. CERN-EP/83-135 (unpublished).

[9]R. D. Feynman, R. P. Field, and G. C. Fox, Nucl. Phys. **B128**, 1 (1977); R. P. Field and R. D. Feynman, Phys. Rev. D **15**, 2590 (1977); Nucl. Phys. **B136**, 1 (1978).

[10]G. C. Fox and R. Kelly, Caltech Report No. CALT-68-890, 1982 (unpublished); R. D. Field, G. C. Fox, and R. L. Kelly, Phys. Lett. **119B**, 439 (1982); R. D. Field and G. C. Fox, University of Florida Report No. UFTP-82-30, 1982 (unpublished).

[11]R. Odorico, Phys. Lett. **118B**, 151 (1982).

[12]R. Singer, T. Fields, and W. Selove, Phys. Rev. D **25**, 2451 (1982).

[13]M. Glück, E. Hoffman, and E. Reya, Z. Phys. C **13**, 119 (1982); J. Owens (private communication).

[14]J. K. Yoh *et al.*, Phys. Rev. Lett. **41**, 684 (1978); L. M. Lederman, in *Proceedings of the 19th International Conference on High Energy Physics, Tokyo, 1978,* edited by S. Homma, M. Kawaguchi, and H. Miyazawa (Phys. Soc. of Japan, Tokyo, 1979), p. 706; K. J. Anderson *et al.*, Phys. Rev. Lett. **42**, 944 (1979).

[15]G. Hanson *et al.*, Phys. Rev. D **26**, 991 (1982); Gunter Wolf, Report No. DESY 80/85, 1980 (unpublished); TASSO collaboration, Report No. DESY 79/73, 1980 (unpublished).

[16]The DESY PETRA data clearly shows that the average value of p_T with respect to the jet axis (q_T) increases as the center-of-mass energy increases. We have not included this increase in the Monte Carlo, but have fixed the value of $\langle q_T \rangle$ at SLAC SPEAR values. Allowing $\langle q_T \rangle$ to increase with parton momentum would result in softer beam and target jets, which would increase $d\sigma/dE_T$ and perhaps decrease planarity.

[17]T. Sjöstrand *et al.*, University of Lund Report No. LUTP-80-3 (unpublished); B. Andersson *et al.*, Phys. Rep. **97**, 31 (1983).

[18]T. Åkesson and H. U. Bengtsson, Phys. Lett. **120B**, 233 (1983).

[19]H. E. Miettinen, Phys. Rev. D **27**, 2236 (1983).

[20]R. D. Field and K. A. Johns (private communication).